Publication I

I. Aaltio, M. Lahelin, O. Söderberg, O. Heczko, B. Löfgren, Y. Ge, J. Seppälä, and S.-P. Hannula. 2008. Temperature dependence of the damping properties of Ni–Mn–Ga alloys. Materials Science and Engineering A, volumes 481-482, pages 314-317.

ELSEVIER

Materials Science and Engineering A 481–482 (2008) 314–317

MATERIALS SCIENCE & ENGINEERING A

www.elsevier.com/locate/msea

Temperature dependence of the damping properties of Ni–Mn–Ga alloys

I. Aaltio [a,*], M. Lahelin [b], O. Söderberg [a], O. Heczko [a], B. Löfgren [b], Y. Ge [a], J. Seppälä [b], S.-P. Hannula [a]

[a] *Laboratory of Materials Science, Helsinki University of Technology, Vuorimiehentie 2A, P.O. Box 6200, FI-02015 TKK, Espoo, Finland*
[b] *Laboratory of Polymer Technology, Helsinki University of Technology, Kemistintie 1, P.O. Box 6100, FI-02015 TKK, Espoo, Finland*

Received 17 May 2006; received in revised form 29 November 2006; accepted 10 December 2006

Abstract

Single-crystalline 5M (exhibiting magnetic shape memory effect) and non-modulated martensitic Ni–Mn–Ga alloys were studied by dynamic mechanical analysis (DMA) at different temperatures. The chemical compositions of the alloys were determined using energy-dispersive X-ray spectrometry in a scanning electron microscope. The crystal structures were confirmed with X-ray diffraction and the transformation temperatures were measured. DMA measurements showed that the mechanical modulus (stiffness) and damping capacity increased during heating and a clear peak of the loss angle, was detected which is related to the reverse phase transformation of martensite to austenite. During cooling, there is a corresponding peak related to the martensite reaction. Significant decrease of the damping capacity occurs during transformation to austenite. Enhanced damping in the martensitic phase can be attributed to the mobility of twin boundaries.

Keywords: Ni–Mn–Ga alloy; Ferromagnetic martensite; Magnetic shape memory effect; Vibration damping; Dynamic mechanical analysis (DMA)

1. Introduction

The vibration damping of a structure can be achieved by active damping that senses and suppresses vibrations in real time or by passive damping structures and materials that absorb the vibrational energy [1]. The components of the vibration damping structures are selected among the materials exhibiting high damping capacity including a large selection of high damping metallic materials [2]. Good vibration damping in metals is related to the microstructure. In shape memory alloys (SMAs), the dissipative motion of the different phases and twin boundaries [1,3] absorb the external vibrations. In ferromagnetic alloys the magnetomechanical damping may base on the hysteretic motion of the magnetic domain walls [4]. Which damping mechanism applies in practice, depends on the damping material, type of the external vibration (frequency, waveform, amplitude), the service temperature and other external factors (loads, chemical activity, etc.).

The microstructure of the ferromagnetic, twinned martensite in magnetic shape memory alloys (MSMAs) consists both of the martensitic twins and of the magnetic domains. The most common MSMAs, Ni–Mn–Ga alloys, exhibit usually the conventional thermally triggered shape memory effect (SME) [5], while some of them show superelasticity, i.e. the stress-induced martensite formation at a certain temperature region above the reverse transformation [6–8]. Also rubber-like behavior has been recently reported [9], which may have an influence on the damping properties. In some Ni–Mn–Ga alloys the magnetic-field-assisted superelasticity, i.e., totally recoverable stress-induced deformation in a constant magnetic field, is present [6,10]. All these phenomena can promote the damping ability of the Ni–Mn–Ga alloys.

The damping of bulk samples has been studied with quasi-static mechanical testing under tensile and compressive loading. The polycrystalline $Ni_{51}Mn_{28}Ga_{19}$ (number indicate at.%) [11] gave for $\tan\delta = 0.4925$ and for elastic modulus $E = 7.8$ GPa. In the single-crystalline $Ni_{50}Mn_{29}Ga_{21}$ [12] $\tan\delta$ increases with increasing maximum strain level at room temperature. Its damping capacity depended also on the amount of the loading cycles. Consequently, the $\tan\delta$ values as a function of energy can be considered average measurements of damping. The observed damping properties were comparable with general viscoelastic materials (VEMs).

Damping can also be studied by dynamic mechanical analysis (DMA), which is traditionally a standard method in polymer analysis. DMA is very sensitive to changes in material properties

* Corresponding author. Tel.: +358 9 4512688; fax: +358 9 4512677.
E-mail address: ilkka.aaltio@tkk.fi (I. Aaltio).

0921-5093/$ – see front matter © 2007 Elsevier B.V. All rights reserved.
doi:10.1016/j.msea.2006.12.229

and it has been used to measure the internal friction, modulus and the transformation temperatures for several alloys; for example Ni–Mn–Ga [13–15], Cu–Al–Ni [16] and Fe–Ni [17]. When evaluating damping with the DMA measurements, the most important factors are the phase difference ($\tan\delta$) and loss modulus (E'') [18]. The phase difference ($\tan\delta$) between the sinusoidal applied stress and the resulting strain gives the internal friction of the material. The storage modulus E' is the real part of the complex modulus and represents the elasticity of the material. The loss modulus E'' is the imaginary part of the complex modulus and represents the ability of the material to "lose" energy. In Refs. [13,15] the transformation behavior of single-crystalline alloys $Ni_{51.1}Mn_{24.9}Ga_{24.0}$, $Ni_{51.2}Mn_{31.1}Ga_{17.7}$ and $Ni_{52.6}Mn_{23.6}Ga_{23.8}$ and a polycrystalline $Ni_{58.3}Mn_{15.9}Ga_{25.8}$ were studied with DMA, and softening was observed near the martensitic transformation.

Even though there are several studies applying the DMA for evaluating internal friction of the material, there are just a few studies dealing with the damping of the Ni–Mn–Ga alloys and even less information is available of the damping properties of the alloys suitable for MSM use. Depending on the composition of the Ni–Mn–Ga alloys, they show various martensite phases with different mechanical and transformation behavior. The present study analyses the DMA behavior of several Ni–Mn–Ga alloys exhibiting the five layered (5M) and non-modulated (NM) crystal structure.

2. Experiments

The test materials were produced by directional solidification at Outokumpu Research, Inc. and Adaptamat Ltd., Finland. The ingots were annealed in the vacuum quartz ampoules at 1273 K for 48 h and at 1073 K for 72 h. Rectangular single crystal "stick" shaped samples were cut with spark machining along the ingot length, i.e. the orientation of the cut samples was not determined. The samples were mechanically polished and finally electropolished in 25% HNO_3. The crystal structure was determined by X-ray diffraction at room temperature (Philips X'pert system). Sample A2 had a five-layer (5M) martensite structure, samples A3 and A4 were of non-modulated (NM) martensite and A1 had a mixed martensite structure. The values in Table 1 for the phase transformations were determined by digital scanning calorimeter (Linkam DSC 600) with 4 K/min rate and Curie temperatures of the alloys were determined by a.c. magnetic susceptibility measurements. The chemical compositions in Table 1 were measured by scanning electron microscopy (SEM) and energy-dispersive X-ray microanalysis (EDS).

The damping properties of the alloys were studied by using the Perkin-Elmer Dynamic Mechanical Analyser DMA-7. The configuration used was three-point bending (3pb) with the sample in horizontal position. The dimensions of the rectangular samples varied significantly, and thus, different amount of force had to be applied to achieve high enough amplitude for a quality DMA run. It is possible that this different force level had an effect on the measured modulus. The used 3pb platform effective length and the other sample dimensions are shown in Table 1. The initial applied amplitude was 3–5 μm, and the amplitude was left free during the measurement. The value of $\tan\delta$ is measured as the ratio between loss and storage modulus: $\tan\delta = E''/E'$. The DMA measurements were performed at a fixed 1 Hz frequency at zero magnetic field and the applied temperature range varied depending on the transformation temperatures of the sample. Cooling and heating were carried out with a rate of 4 K/min. The sample was measured when heated up, and the temperature was then kept constant for 3 min before the cooling in order to allow the DMA sample to stabilize before new measurement. Temperature was measured by a thermocouple from a point about 1 mm up and 2–4 mm (depending on the effective length of sample) along the axis from the top of the sample surface. This explains the differences of the temperature dependency of the DMA curves and values in Table 1 as the inner temperature of the sample followed the thermocouple temperature with some delay. The difference is small during heating but larger during cooling. A comparative DMA measurement was also performed for a sample made of pure Ti.

3. Results and discussion

The DMA measurement results are shown in Figs. 1–4, where the storage modulus E', loss modulus E'' and $\tan\delta$ are shown as a function of temperature during heating (denoted by h) and cooling (c). The damping ($\tan\delta$) of all materials is much larger in martensite than in the austenite phase. This is expected, as in austenite, there is no twinning, or any other significant damping mechanism. However, low damping is difficult to measure with the used DMA system, aimed for measurements of high damping capacity.

During the a–m transformation the storage modulus E' of all samples exhibits a decrease at the transformation temperature accompanied by a sharp peak of $\tan\delta$. It is most remarkable in A2 sample (5M) where E' decreases to nearly 1 GPa (Fig. 2).

Table 1
Chemical compositions (at.%), phase transformation and Curie temperatures (K), primary martensite structure and cross-sectional dimensions (mm) of the test materials

Sample	Ni (at.%)	Mn (at.%)	Ga (at.%)	M_s (K)	M_f (K)	A_s (K)	A_f (K)	T_c (K)	Crystal structure of martensite	Effective length × width × thickness (mm^3)
A1	48.9	30.0	21.0	311	297	313	320	375	Mixed	15 × 1.54 × 0.95
A2	49.7	29.1	21.2	307	300	316	320	372	5M	10 × 2.08 × 1.89
A3	55.1	22.1	22.9	374	367	376	386	377	NM	15 × 2.78 × 0.87
A4	52.3	27.4	20.3	407	400	410	418	380	NM	15 × 1.29 × 1.06

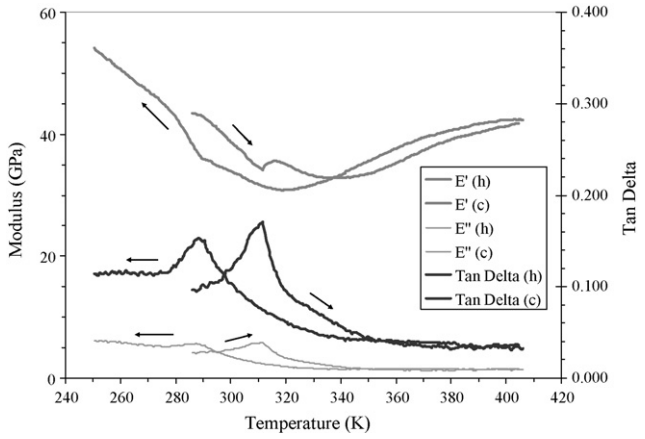

Fig. 1. DMA measurement curves of the sample A1 as a function of temperature.

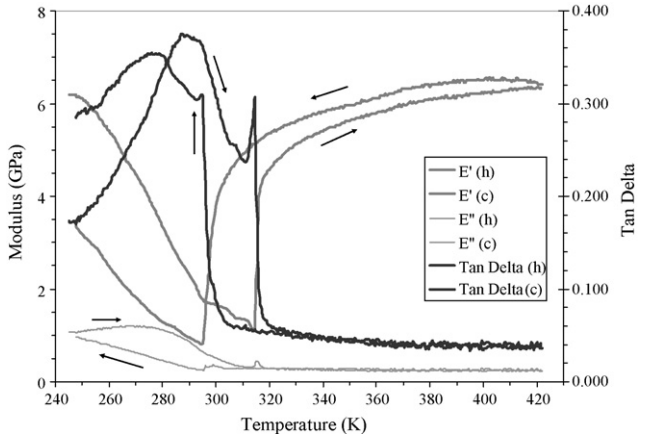

Fig. 2. DMA measurement curves of the sample A2 as a function of temperature.

In all samples, tan δ shows a smaller peak when approaching the m–a transformation during heating. The peaks are a result of the lattice softening (soft mode condensation) during the transformation. Similar observations have been reported earlier [13]. When cooling, a measurement-dependent delay exists as a function of temperature as stated before. We believe that the peak in tan δ denotes the phase transformation even though the DSC indicates a different temperature. The temperature difference is probably a result of the measurement configuration as discussed before. There is no discernible change of damping during ferromagnetic–paramagnetic transformation. This is due to the fact that the magnetic hysteresis in Ni–Mn–Ga is very low [19], and therefore, does not contribute significantly to the damping.

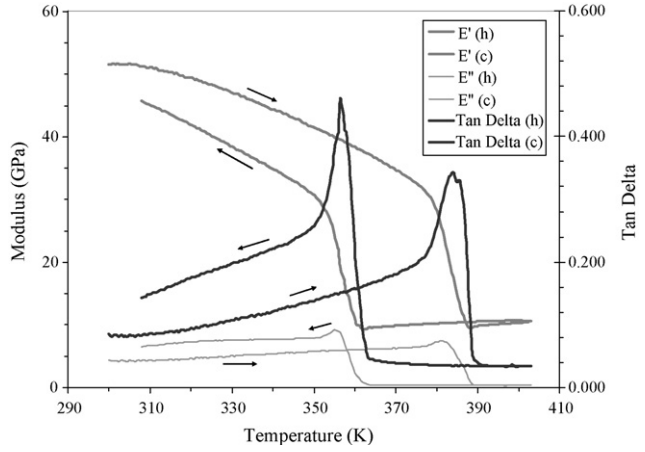

Fig. 3. DMA measurement curves of the sample A3 as a function of temperature.

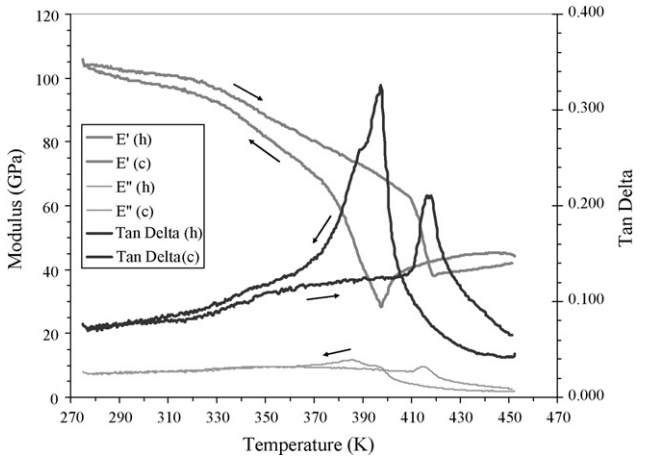

Fig. 4. DMA measurement curves of the sample A4 as a function of temperature.

Loss modulus E'' stays nearly constant in the martensitic phase. However, tan δ decreases because the storage modulus E' clearly increases with decreasing temperature. At m–a transformation there is a small but discernible peak of loss modulus E'', which suggests the increase of the damping due to movable phase boundaries or stress-induced martensite formation. The peak of tan δ is much larger due to the decrease of the storage modulus E'. The values of storage modulus differ sharply ranging from a few GPa to above 100 GPa. This reflects the different martensite structures. In the case of A2 (Fig. 2), tan δ shows more stable levels in the martensite and austenite phases, and the damping of martensite is on a higher level than in other test samples (Figs. 1, 3 and 4). The increased damping in sample A2 is due to high mobility of the twin boundaries in 5M martensite. It is interesting to note that when cooling from austenite after initial peak in tan δ denoting the transformation, there is another broad peak after transformation and then tan δ decreases again. The decrease of tan δ with decreasing temperature reflects the decreasing mobility of twin boundaries with decreasing temperature [19], which is also demonstrated in Fig. 5. It has been shown [20–22] that the twinning stress of martensite and the corresponding hysteretic stress in austenite [22] decreases around the transformation temperatures. Sample A1 and to some extent sample A4 show broad temperature evolution of measured values probably due to sample inhomogeneity. Very sharp transformation in A2 and A3 samples indicate to higher homogeneity and single crystal state. After the DMA thermal cycle, tan δ remains at a higher level compared to the initial value, and differences in E' and E'' exist as well. This may be a result of re-orientation of the martensite structure with the mechanical stress, but this suggestion was not verified.

The compressive mechanical testing has been performed with single-crystalline samples prepared of the A1 ingot to investigate

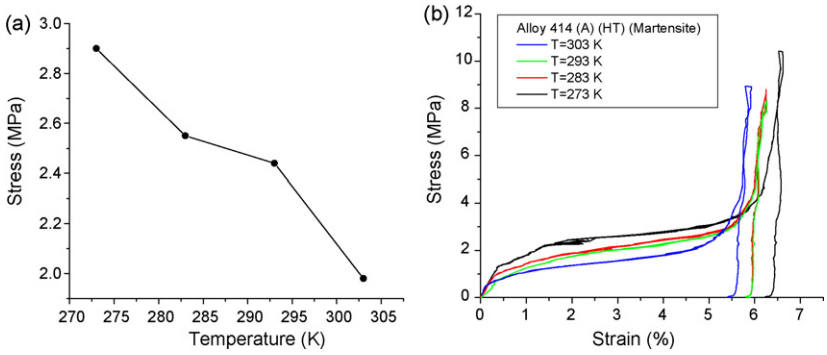

Fig. 5. Twinning stress of A1 (in $H = 0$) determined from the 4.5% strain at different temperatures (left) and the corresponding compression σ–ε-curves (right).

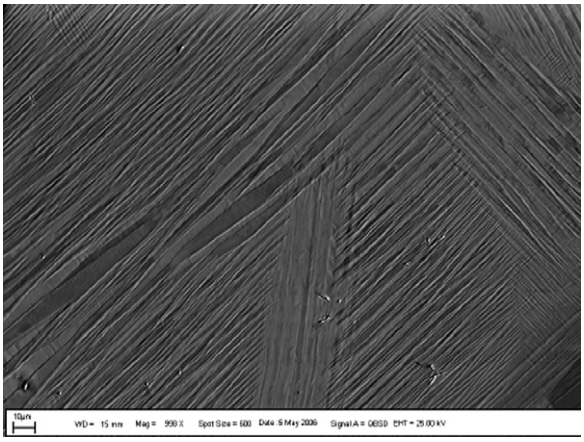

Fig. 6. A scanning electron backscattering micrograph of the sample A1. The Mn content of the inhomogenous sample varied by 2 at.%. The width of the figure corresponds to about 27 μm.

the twinning stress (Fig. 5). These results correlate well with the damping results of Fig. 1, as the decrease of twinning stress and increase of damping are both observed when the sample is heated to about 303 K. This result suggests that the increasing motion of the twin boundaries would dissipate more vibration energy in the material. A micrograph of A1 is shown in Fig. 6, which shows a complex and inhomogeneous martensitic structure. The mechanical testing and damping results should be verified with a more homogenous sample.

4. Conclusions

The tests showed that the values of tan δ of the martensitic Ni–Mn–Ga alloys are relatively high (up to 0.35), and they strongly vary with temperature, possibly reflecting the mobility of twin and phase boundaries. The peak of damping occurs at the martensitic transformation. The 5M martensite sample has the highest damping values (tan δ) of the tested samples, but tan δ decreases at a lower temperature compared to tan δ of the NM or mixed martensite samples. NM samples exhibit relatively high damping up to 373 K when heating. More comprehensive internal friction tests would be needed in order to find the dominating damping mechanisms.

Acknowledgements

Kari Koho and Jarkko Vimpari are thanked for performing the measurements of Fig. 5 and Natalia Lanska is acknowledged for the determination of the martensite structure by X-ray diffraction. We thank the Finnish Funding Agency for Technology and Innovation (Tekes) and the Academy of Finland for their support.

References

[1] ChungF D.D.L., J. Mater. Sci. 36 (2001) 5733–5737.
[2] M.F. Ashby, Materials Selection in Mechanical Design, Butterworth-Heinemann, Oxford, 1999, p. 502.
[3] I. Aaltio, K. Ullakko, Smart Mater. Struct. 6 (1997) 616–618.
[4] I. Aaltio, K. Ullakko, H Hanninen, Proceedings of The SPIE Symposium on Smart Structures and Materials, vol. 2720, 1996, p. 378.
[5] O. Söderberg, Y. Ge, A. Sozinov, S.-P. Hannula, V.K. Lindroos, in: J. Buschow (Ed.), Handbook of Magnetic Materials, vol. 16, Elsevier Science, Amsterdam, 2006, pp. 1–39.
[6] V.A. Chernenko, V. L'Vov, J. Pons, E. Cesari, J. Appl. Phys. 93 (2003) 2394–2399.
[7] O. Heczko, V.A. L'vov, L. Straka, S.-P. Hannula, J. Magn. Magn. Mater. 302 (2006) 387–390.
[8] O. Heczko, L. Straka, Mater. Sci. Eng. A 378 (2004) 394–398.
[9] I. Glavatskyy N. Glavatska, Mater. Sci. Eng. A, 10th Int. Symp. Physics of Materials ISPMA-10, Prague, 30 Aug – 2 Sep 2005.
[10] L. Straka, O. Heczko, IEEE Trans. Magn. 39 (2003) 3402–3404.
[11] D.A. Ruggles, E. Gans, K.P. Mohanchandra, G.P. Carman, E. Ngo, W. Nothwang, M.W. Cole, Proc. SPIE-Int. Soc. Opt. Eng. 5387 (2004) 156–163.
[12] E. Gans, C.G. Henry, Active Mater.: Behav. Mech. (2004) 177–185.
[13] C. Segui, E. Cesari, J. Pons, V. Chernenko, Mater. Sci. Eng. A 370 (2004) 481–484.
[14] C. Segui, E. Cesari, J. Font, J. Muntasell, V.A. Chernenko, Scripta. Mater. 53 (2005) 315–318.
[15] C. Segui, V.A. Chernenko, J. Pons, E. Cesari, V. Khovailo, T. Takagi, Acta Mater. 53 (2005) 111–120.
[16] N. Suresh, U. Ramamurty, Smart Mater. Struct. 14 (2005) N47–N51.
[17] H. Wang, J. Zhang, T.Y. Hsu, Mater. Sci. Eng. A 380 (2004) 408–413.
[18] A.K. Sircar, in: E.A. Turi (Ed.), Thermal Characterization of Polymeric Materials, vol. l, Academic Press, New York, 1997, pp. 887–1378.
[19] O. Heczko, L. Straka, J. Appl. Phys. 94 (2003) 7139–7143.
[20] K. Koho, J. Vimpari, L. Straka, N. Lanska, O. Soderberg, O. Heczko, K. Ullakko, V.K. Lindroos, J. Phys. IV 112 (2003) 943–946.
[21] L. Dai, J. Cullen, J. Cui, M. Wuttig, Mater. Res. Soc. Symp. Proc. 785 (2004) 47–56.
[22] I. Aaltio, J. Tellinen, K. Ullakko, S.-P. Hannula, H. Borgmann (Eds.), Proc. of ACTUATOR, Bremen, Germany, 2006, pp. 402–405.